Experimental Comparison on the Energy Performance of Semi-Transparent PV Facades Under Continental Climate

Zissis Ioannidis[1], Konstantinos Kapsis[1], Annamaria Buonomano, Andreas Athienitis[1,] Eftsratios Dimitrios Rounis[1] and Ted Stathopoulos[1]

[1] Dept. of Building, Civil and Environmental Engineering, Concordia University, Montreal (Canada)

[2] *Department of Industrial Engineering, University of Naples Federico II, Naples, (Italy)*

Abstract

Semi-Transparent Photovoltaic panels (STPV) have become an important element in the building integration of photovoltaic panels (BIPV). STPV panels can be integrated on double skin facades (DSF) and insulating glazing units (IGU) acting as their exterior layer, generating electricity, controlling the solar heat gains and utilizing daylight. In addition, a mechanically ventilated DSF integrating STPV panels (DSF-PV), can cool down the PV panels, increase their efficiency but also use the preheated air to enhance the thermal efficiency of the mechanical system connected to the DSF-PV. Two virtually identical STPV are integrated on a DSF-PV and a IGU-PV respectively and their electrical performance is evaluated experimentally. Under the same exterior and interior conditions, it is found that the DSF-PV has a 3% greater electrical performance than the IGU-PV and if the cavity of the DSF-PV is selectively ventilated, the DSF-PV can generate more than 9% of electric power than the IGU-PV.

Keywords: Double Skin Façade, IGU, STPV, BIPV, BIPV/T, Semi-Transparent, PV

1. Introduction

It is very common for both commercial and residential modern buildings to use curtain wall systems as part of their envelope design. A well-designed curtain wall system is able to seal the building, protect it from weather phenomena and provide to the building the modern architectural aesthetics. The large transparent facades are preferred due to the reduced cost and the great appreciation of daylighting, as the sun light can penetrate deeper into the building. This architectural tendency is likely to remain, due to the low cost of the curtainwall application and the fact that more studies link daylight and view to the outdoors with increased worker productivity, well-being (Veitch and Galasiu 2011) and reduced lighting loads (Tzempelikos and Athienitis 2007). Highly glazed facades may maximize the daylight potentials of the building but they may require an oversized mechanical system, as excessive solar gains may lead to increased cooling loads during the day and low insulation may lead to increased heating loads during the night, adding to the thermal and visual discomfort of the occupants.

The disadvantages of highly glazed facades may be minimized or overcome by either integrating photovoltaics (PV) on windows or by adding an additional exterior layer forming in this way a double skin façade (Miyazaki, Akisawa, and Kashiwagi 2005). Solar cells may be used instead of reflective coating or ceramic frits to reduce the solar gains, forming in this way semi-transparent photovoltaics (STPV) that could be integrated on parts of the façade of the building (James, Jentsch, and Bahaj 2009; Qiu et al. 2009). As a result, solar heat gains may be reduced, maintaining at the same time adequate levels of daylight, provide view to the outdoors (Vartiainen 2001) and generate electricity.

When PV cell overheating is of concern, instead of a window with a sealed cavity (IGU), a ventilated one can be utilized, turning the façade into a Double Skin Façade integrating photovoltaics (DSF-PV). The possibility of recovering the heat from within the DSF-PV, along with the electricity generation and the daylight transmission, gives the opportunity to the creation of an active façade (Gaillard, Giroux-Julien, et al. 2014). As the air circulates behind the PV cells, it cools down the cells through convection, reducing the temperature of the cells and increasing their

doi:10.18086/swc.2017.12.04 Available at http://proceedings.ises.org

electrical efficiency.

STPV façades could have a substantial effect on the daylighting/lighting performance as well as energy and peak power demand reduction on highly-glazed office buildings. The objective of this study is to experimentally investigate the energy performance of two prevailing STPV façade configurations: i) curtain wall systems incorporating STPV insulated glazing units (IGU-PV), ii) Double Skin Façade incorporating STPV technologies on the outer skin (DSF-PV). The study focuses on offices in a continental climate region (Northeastern United States and Southeastern Canada) and it is part of a bigger effort to provide input to the design guidelines for the utilization of advance fenestration technologies that will help to achieve net-zero energy building performance targets and beyond, through energy conservation and renewable energy generation.

2. Literature review on experimental investigation

A series of experiments have been held to characterize the performance of windows and double skin facades integrating photovoltaic panels. Single, double and ventilated windows have been investigated, while the majority of the studies used amorphous silicon (a-Si) photovoltaic panels. The experiments were mainly focused on the electrical performance of the integrated photovoltaics, but many studies focus as well on the thermal and daylight performance of such systems.

2.1 Windows integrating Photovoltaic

To assess the electrical performance of amorphous silicon STPV modules, the Sandia model was first validated experimentally by Peng et al, with indoors and outdoors experiments (Peng et al. 2015b). It is reported that Sandia model is able to predict the electrical output of the STPV modules on a sunny day but in order to predict the electricity production on an overcast day a spectral correction should be applied to correctly simulate the performance of the STPV windows. It is reported that a comprehensive spectral correction function is needed to be developed in the future.

An experiment was set-up by Robinson and Athienitis (2009), integrating STPV on a double glazing window in Montreal (Robinson and Athienitis 2009) focusing on its electrical and daylight performance. A design methodology for optimizing the electricity generation and the daylight utilization was validated showing the potentials of south facing STPV facades.

In addition to the electrical performance, the thermal performance of a double glazing STPV module was studied under standard test conditions and outdoor conditions (Park et al. 2010). For an increase of 1^{o}C of the PV module, it is observed that the temperature coefficient (β) is 4.8% and 5.2% under STC and outdoor conditions respectively (irradiance of 500W/m^2). It is also reported that the type of glass used at the STPV window does not affect the electrical performance of the module but affects the thermal performance of the system.

A comparison is held between an a-Si STPV double glazing unit and common single and double glazing units in terms of their electrical and thermal performance (Liao and Xu 2015). Liao and Xu focused mainly on the room and façade dimensions to develop a model and later validate it with field experiments in order to simulate it with the use of Energy Plus. Amorphous silicon STPV windows are found to be better suited for small rooms with high WWR or tall rooms. It is also found that they perform better than single and double-glazing units, mainly because they reduce the cooling loads of the interior zone.

The SHGC of STPV modules and STPV windows was measured using a calorimetric box in a solar simulator (Chen et al. 2012). Three laminated and two double glazing units with amorphous and micromorph are tested in the Solar Simulator and it is reported that it is sensitive to the spectrum of the solar simulator and the reflection properties of the absorber plate. It is also reported that the SHGC reduces significantly for incident angles greater than 45^{o}.

In addition, a hot-box is used by He et al. (He et al. 2011) to compare an amorphous single-glazing PV window to a ventilated double-glazing PV window. With an electrical efficiency of less than 5% and with a packing factor of 0.8 the SHGC of the IGU integrating STPV is 46.5% in comparison to the single glazing STPV. A CFD analysis is held using ANSYS FLUENT and RNG k-epsilon turbulence model. The difference between the experiments and the model created, for the total heat gains, is 11.7% and 2.7% for the ventilated double-glazing PV window and the single-glazing respectively and the estimated temperature difference is less than a degree C for both cases.

A ventilated thin-film PV window is experimentally assessed and verified using a developed ESP-r simulation model that is then used to compare the STPV window with a simple absorptive glazing (Chow, Qiu, and Li 2009). For an electrical efficiency of less than 5%, the STPV window is compared to an a-Si STPV product available in the market and an to absorptive glazing. It is shown that the see-through PV installation can reduce the consumption of the HVAC by 28%.

An exterior experimental facility was set up by Olivieri et al (2013), to assess the electrical, thermal and daylighting and behavior of an STPV window (Olivieri et al. 2014). It is reported that the transparency of the PV window is not the most important factor concerning the electrical performance. Four a-Si STPV modules with visible transmittances between 0.1 and 0.4 have been experimentally compared to a reference glass. All four modules present higher SHGC, approximately 40% larger heat losses and the U-values are almost double in comparison to the reference glass.

The optimal packing factor of STPV windows for office buildings in central China was investigated, for different room lengths, WWRs and orientations (Xu et al. 2014), analyzing its electrical, thermal and daylighting performance. A parametric analysis is performed, using Energy Plus, to identify the impact of different cell coverages into the energy consumption of the zone, stating that the selection of the optimal configuration can reduce the energy consumption up to 13% in comparison to the least favorable configuration.

2.2 Double Skin Facades integrating Photovoltaic

The integration of PV on DSF is an idea that has recently received the attention of the academic community. The majority of the research is focused on naturally ventilated DSF integrating STPV made out of amorphous silicon.

Peng et al, set-up an experimental facility in Hong Kong, consisting of a DSF integrating see-through a-Si PV (Peng et al. 2015a; Peng, Lu, and Yang 2013). The DSF has a cavity width of 400mm that is created between a double glazed see-through PV and the interior window and inlets at the top and the bottom, both at the exterior side. Four different operation modes of the dampers and the interior window were experimentally investigated showing that the temperature of the air at the outlet can be more than 2ºC higher than the one at the inlet. It is also reported that the SHGC for the different operation modes are between 0.1 and 0.13.

The same experimental facility was later used to validate a developed simulation model, based Energy Plus (Peng et al. 2016). For a cool-summer Mediterranean climate zone, a thickness between 0.4m and 0.6m could be recommended as the optimal cavity width while the DSF-PV, used 50% less net-electricity than other glazing systems. In addition, it is highlighted that the future of the DSF-PV is promising because of the decrease of the prices and the increase of the efficiencies of the PVs.

Three prototype DSFs integrating semi-transparent photovoltaics are tested and a comparison between the thermal response of the semi-transparent photovoltaics and the air inside the cavity is presented (Gaillard, Ménézo, et al. 2014). The two-storey West North-West DSF of the building is designed to increase the electrical performance of the semi-transparent photovoltaics installed by utilizing the stack effect (Gaillard, Giroux-Julien, et al. 2014). As reported by the experimental data collected under real conditions, in a span of a year, the behavior of the system can be predicted by using simple relationships.

An experimental facility was built in Hong Kong to compare the energy performance of a Double Skin Façade (DSF) and an insulation glass unit (IGU) integrating semi-transparent photovoltaics (Wang et al. 2017). The thermal

performance of the IGU integrating STPV was found to be better by 2% than the naturally ventilated DSF integrating photovoltaics (DSF-PV), although the authors mentioned that an appropriate ventilating mode for the DSF-PV would potentially result into better thermal performance.

In Table 1, the available state of the art is shown, presenting the experimental research performed on windows and double skin facades integrating semi-transparent photovoltaics. The available literature is also analysed presenting the different type of PV utilized, the types of windows used and whether the DSF is mechanically or naturally ventilated. In addition, the focus of the study is presented along with whether any simulation models are used. The last row states the location of the experimental facility, if it is an exterior one, or if the experiments are performed on a solar simulator.

Table 1 Available literature on experimental research perfromed on windows and DSF integrating PVs

Study	PV				Window				DSF		Focus			Simulation				Location
	a-Si	Mono-Crystaline	Poly-Crystalline	Micromorph	Single	Double	Triple	Ventilated	Mechanically ventilated	Naturally Ventilated	Electrical	Thermal	Daylighting	Numerical model	Energy Plus	ESP-r	CFD	
J. Peng et al (2015)	✓										✓							Solar Simulator
L.Robinson and A.Athienitis (2009)			✓			✓					✓		✓	✓				Montreal
K. E. Park et al (2010)			✓			✓					✓	✓						Solar Simulator
W. Liao and S. Xu (2015)	✓					✓					✓	✓		✓	✓			
F. Chen et al. (2012)	✓			✓	✓	✓					✓	✓						Solar Simulator
W. He et al (2011)	✓				✓	✓		✓			✓	✓					✓	Hefei
T. T. Chow et al (2009)	✓							✓			✓	✓				✓		Hong Kong
Olivieri et al (2014)	✓				✓						✓	✓	✓					Madrid
S. Xu et al (2014)					✓						✓	✓	✓		✓			Wuhan
J. Peng et al (2013)	✓									✓		✓						Hong Kong
L. Gaillard et al (2014)			✓							✓		✓		✓				Toulouse
J. Peng et al (2015)	✓									✓	✓	✓						Hong Kong
M. Wang et al (2017)	✓					✓				✓	✓	✓	✓		✓			Hong Kong

Based on the Mataro Library in Barcelona, Mei et al, developed a dynamic thermal model on TRNSYS for a DSF integrating STPV (Mei et al. 2003). For a 15% transparency and an assumed as constant transmittance-absorptance of 0.8 STPV panel a thermal model was developed. It is reported that the air at the outlet of the DSF-STPV can reach

50°C in summer and 40°C in winter and this preheated air can be introduced into the HVAC system to reduce the heating load by 12%. Based on the same building the potential to use a desiccant cooling machine in combination with the DSF-PV is investigated (Mei et al. 2006). The 70°C heated air within the DSF can be fed into the desiccant cooling machine and regenerate the sorption wheel, resulting into an average COP of 0.518 during the summer season. The approach of four different terms describing the ventilation gains, the transmission losses and the temperature components are used in a steady state analysis to simulate the Mataro Library DSF-PV (Infield, Mei, and Eicker 2004) (Infield et al. 2006). In this way, monthly U and g values have been derived and the energy thermal gains have been calculated.

An integral (electrical, thermal and daylight) simulation model is used to carry out an annual performance study for an architype office building located at Toronto, Canada (Kapsis and Athienitis 2015). The model is experimentally-verified. The analysis demonstrates that the use of STPV façades have the ability to generate enough electricity to cover the annual electricity demand of the building on electric lighting and plug loads. In case of STPV/T or double skin façade, a significant amount of heat (in the form of preheated outdoor air) could be also generated. The heated air could be used to a solar assisted air-source heat pump that could be used to partially cover the heating and cooling demands of the building. Moreover, the use of STPV/T or double skin façade reduces the heat losses through the building skin during the heating season.

3. Experimental set-up

Two virtually identical semi-transparent photovoltaics (STPV) are used for this experimental set-up, located in Montreal, Canada (45° 30' N / 73° 35' W). The first STPV is used as the exterior layer of a DSF forming in this way a DSF-PV and the second one is used as the exterior layer of an Insulating Glazing Unit (IGU-PV). For each STPV, 48 cells of 17.80% nominal efficiency are used and are distributed in 8 rows with 6 cells in each row. In Figure 1, the experimental test cell is presented, showing the IGU-PV on the left side and the DSF-PV on the right. An automated damper with a Belimo actuator (0-5V) is integrated underneath the DSF-PV and is controlled to ventilate the DSF-PV. The test cell faces towards the south, while the south view of the façade is shown on the panoramic picture of Figure 1. It can be seen that most of the days of the year, the sky-scraper at the east, south-east shades the test cell, in the early morning and for a couple hours after the solar noon the test cell is shaded by the building that is located at the south, south-west.

The characteristics of the STPV modules are presented in Table 2 and the layers of the first and the second STPV are show in Figure 2. Both the STPV have the same layers: glass, Ethylene-vinyl Acetate (EVA), PV cells, EVA and glass. The dimensions of both the STPV panels is 1.968m by 0.992m and the PV cells used are square and have sides of 15.6cm, while the seven transparent strips have a width of approximately 10.3cm. In this way, 63.4% of the area is covered by the cells and the remaining 36.6% is transparent. The insulating glazing unit is assembled with a hard low emissivity coating at the back of the STPV. The space between the STPV and the double glazing is vacuum and 13mm wide.

The cavity of the DSF-PV is 17cm wide and the back layer of the DSF-PV extends from the bottom of the test-cell to a height of 1.90m. The top of the DSF-PV is sealed and a plenum is used to collect the air and drive it through a manifold (Figure 3). A rectangle FLST 25.4cm by 25.4cm (10in by 10in) flow meter by Dwyer is flashed at the middle of this manifold and its location is selected to be at distance from previous and later elbows that could affect the flow.

Both the systems are integrated on the test-cell using mullions and pressure plates that are mainly used in curtainwall applications. On the interior side of the DSF-PV, the double glazing that is used as the interior layer of the DSF-PV, is mounted following the same principal. In this way, the mullion in its width acts as the spacer between the internal and external layer of the DSF-PV and makes it easy for the integration on buildings.

Thermocouples (T-type) are place on the interior side of the STPV and on both sides of the clear IGU of the DSF-PV. In addition, thermocouples are placed in the middle of the cavity, approximately 8.75cm from each side and in the vertical direction. The thermocouples are placed at the same heights in all layers and are evenly distributed along the

height of the DSF-PV (Figure 3). Because the dampers are located underneath the exterior layer of the DSF-PV, the thermocouples on the DSF-PV start at the second height level. Similarly, because of the manifold, the thermocouples on the interior layer stop before the last height level. In Figure 3, all sixteen of the height levels of the thermocouples are shown with each color indicating a different layer.

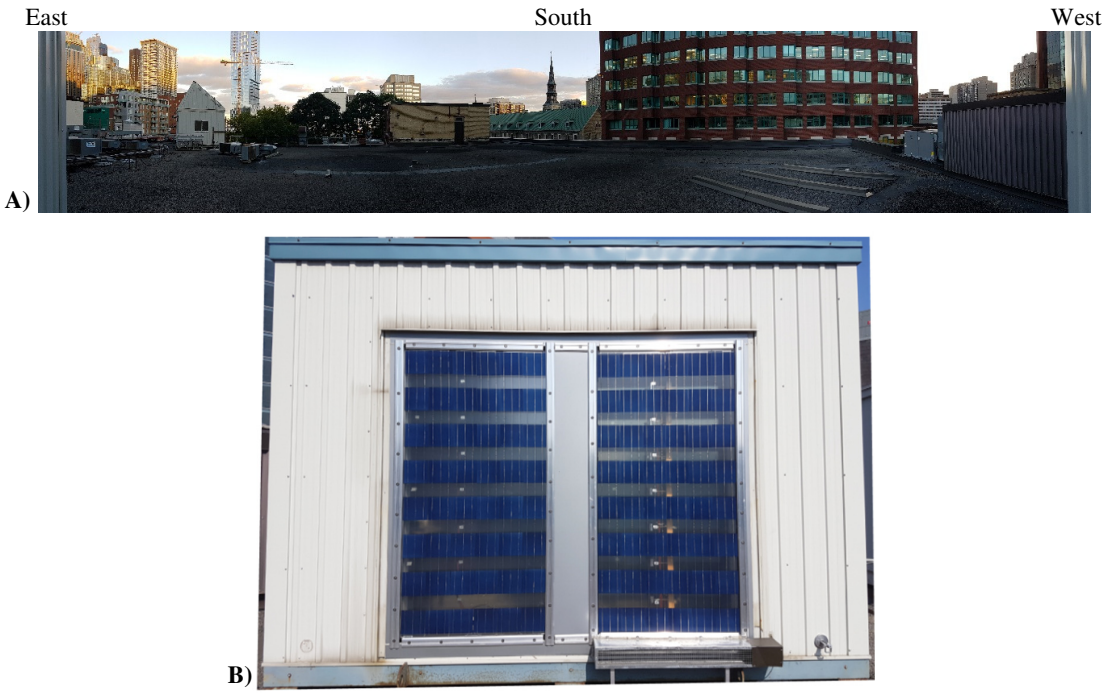

Figure 1 A) View from the south façade of the test-cell, where the STPV are integrated. B) The IGU-PV is installed on the left and the DSF-PV is on the right. The mechanical dampers are shown under the DSF-PV installation.

Table 2 Electrical data of the STPV integrated on the DSF-PV and the IGU-PV

	STPV #1 (DSF-PV)	STPV #2 (IGU-PV)
I_{sc}	8.55 A	8.57 A
V_{oc}	29.90 V	29.98 V
P_{max}	186.39 W	187.95 W
eff	10.6 %	10.7 %
		*under Standard Test Conditions

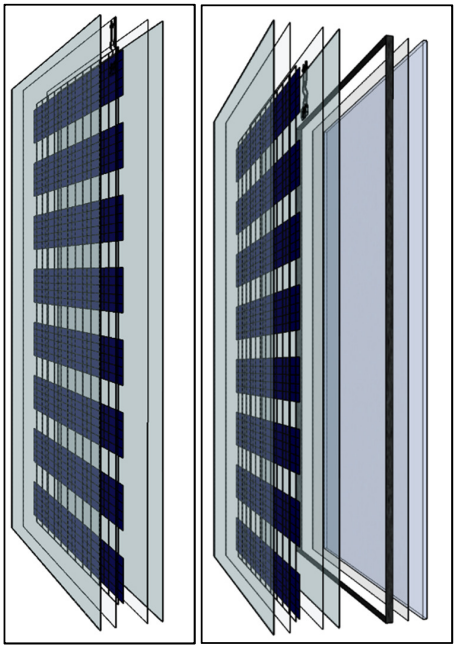

Figure 3 Layers of the STPV used at the DSF-PV (Left) and of the IGU-PV (Right).

Figure 3 Thermocouples are placed on four layers on the DSF-PV (Left) and on the IGU-PV (Right).

For the IGU-PV, thermocouples were installed on the side of the IGU that faces the room, distributed in the same way as they are on the DSF-PV. The data acquisition system used is the LabView using national instruments (NI). For the thermocouples the NI 9213 module is used (National-Instruments 2016). For the accurate measurement of the power output of the DSF-PV and the IGU-PV, an identical electric assembly was set up for each PV module. This assembly consist of a charge controller with maximum power point tracker (MPPT) a battery of 12 V and 110 Ah and a dump load (TE Connectivity 2005). The multi-stage MPPT solar charge controllers used are the Solar Boost SB3024i (Blue Sky Energy Inc. 2009) and the battery is the 8A31DT AGM sealed (MK Battery 2015). The voltage of each PV module is measured with a NI 9223 module (National Instruments 2016) and a shunt resistor (Riedon Inc. 2018) is used to measure the current flowing from the PV. The electrical configuration and connections are shown in Figure 4. The selection of shut resistor was based on the range and precision of the voltmeter. In our case a NI 9213 was used to measure the voltage difference (range of $\pm$78 mV) and using a safety factor of two (2) over the short circuit current from the PV ($\sim$16 A), the value of the shunt resistor was calculated to be 5 mΩ. For the selection of the battery, an empirical rule was used to calculate the battery capacity (Ah), which is equal to the watt peak of the STPV multiplied by the daily solar exposure and the days of battery autonomy of the system, divided by the battery loss factor, the depth of discharge and the battery voltage. In order the MPPT to supply the battery with the maximum current possible, the battery should not be full and this is why a single day of battery autonomy was preferred. Assuming that the PV average daily solar exposure is three hours, the battery loss is 0.85 and the depth of discharge is 0.5 the battery capacity is calculated to be approximately 110 Ah. A resistor is used as dump load to release, in the form of heat, the total electricity generated by the STPV and stored at the battery, during the night, when the heating loads from the resistors will not interact with the STPV experiments. For a 1 Ω resistor and a 12 V battery supply, a 144 W resistor should be used, instead a 300 W resistor was selected to avoid the overheating of the resistor.

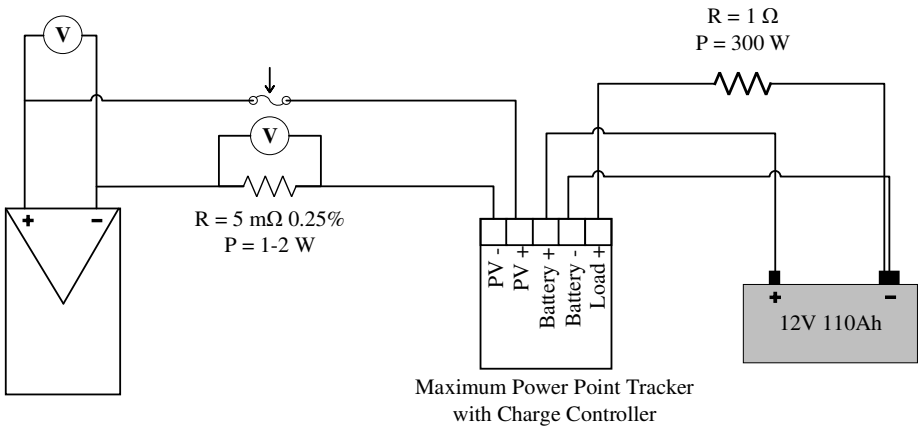

Figure 4 Schematic showing the electrical connection between the STPV, the MPPT and the batteries. The location of the shunt resistors used for the current measurement and the resistors used as a dump load is shown.

4. Experiments and result discussion

The test-cell and the experimental set-up described earlier, is used to characterize the electrical performance of the DSF-PV and the IGU-PV. In addition, a comparison is held between their performance under the same exterior and interior condition.

Experiments that are presented in this paper are for a series of eight (8) consecutive days, under different weather conditions and under different ventilation strategies for the cavity of the DSF-PV. The average velocity within the cavity and the incident solar radiation for these days are presented in Table 3. From Table 3, it can be extracted that for all the monitored days, the DSF-PV out-performs the IGU-PV by a 3% to 10% difference, depending on the strategy selected for the ventilation of the cavity of the DSF-PV.

From the same table, it can be seen that clear sky days are Day 1,4,6,7 and 8 and the overcast days are Day 2, 3, 5. If the cavity is ventilated, the electricity production of the STPV integrated on the DSF is greater than this of the IGU-PV by 7.27% to 9.20%. The days that the cavity is ventilated but the sky is overcast (Day 2 and 3), the electrical performance of the DSF-PV is approximately 4.5% greater than the IGU-PV. Lastly, when the cavity is closed, the difference between the electricity generated by both the STPV, is the smallest encountered but is still between 3.6% and 4.1%. On the last column of Table 3, the percentage of the time that the power of the DSF-PV is greater than the Power of the IGU-PV is presented showing that more than 87% of the time, the DSF-PV performs better than IGU-PV

In Figure 5, a comparison of the power produced and the current generated by the DSF-PV and the IGU-PV is depicted for Day 1 between 7:00 AM and 2:40 PM. The shaded with different colors zones, represent time-periods where different average velocities within the cavity were measured, due to different fan operation.
As it can be seen, the power generation between 7:30AM and 8:00AM drops and this is because of the shading that is provided to the test-cell by the sky-scraper presented in Figure 1. For the same reason, the power drops after 2:15PM, where the building located at the south-west shades the test-cell. The power of the IGU-PV drops first, as it is located on the west side of the test-cell.
When the cavity of the DSF-PV starts to be ventilated, the power generated by the DSF-PV starts to be greater that this of the IGU-PV. The current generated by both the STPVs is almost identical, and this is because the STPV are similar and under the same incident solar radiation. On the other hand, the difference of the power generated by the integrated STPVs should be correlated to the voltage difference created by each system and thus the temperature their cells, as the operating voltage of the STPV panels is dependent on the temperature of the cells.

For the same day (Day 1), the power generated by the DSF-PV and IGU-PV and the voltage at which this power is generated is shown in Figure 6. It can be seen that the DSF-PV operated at a higher voltage of about 2 V than the

IGU-PV. Consequently, the power generated by the DSF-PV is approximately 10 W higher than this of the IGU-PV, for the majority of the time, resulting in the average 9.20% difference presented in Table 3.

Table 3 Experimental data for eight (8) consecutive days in Montreal.

	Average Velocity within the Cavity	Average Incident Solar Radiation (W/m^2/day)	Average diffuse Solar Radiation (W/m^2/day)	Electricity generated by the DSF-PV (Wh/day)	Electricity generated by the IGU-PV (Wh/day)	Daily Difference	Percentage of time $P_{DSF}>P_{IGU}$
Day 1	1.25 m/s	194	44	704.01	644.67	9.20%	96.49
Day 2	0.65 m/s	156	70	561.06	537.31	4.42%	93.81
Day 3	1.10 m/s	156	77	462.91	442.40	4.64%	89.27
Day 4	closed	201	46	637.04	611.58	4.16%	91.24
Day 5	1.20 m/s	170	61	637.62	594.39	7.27%	95.72
Day 6	closed	203	29	754.09	725.23	3.98%	89.85
Day 7	closed	201	25	768.62	741.85	3.61%	87.58
Day 8	1.20 m/s	192	31	742.65	683.23	8.70%	97.72

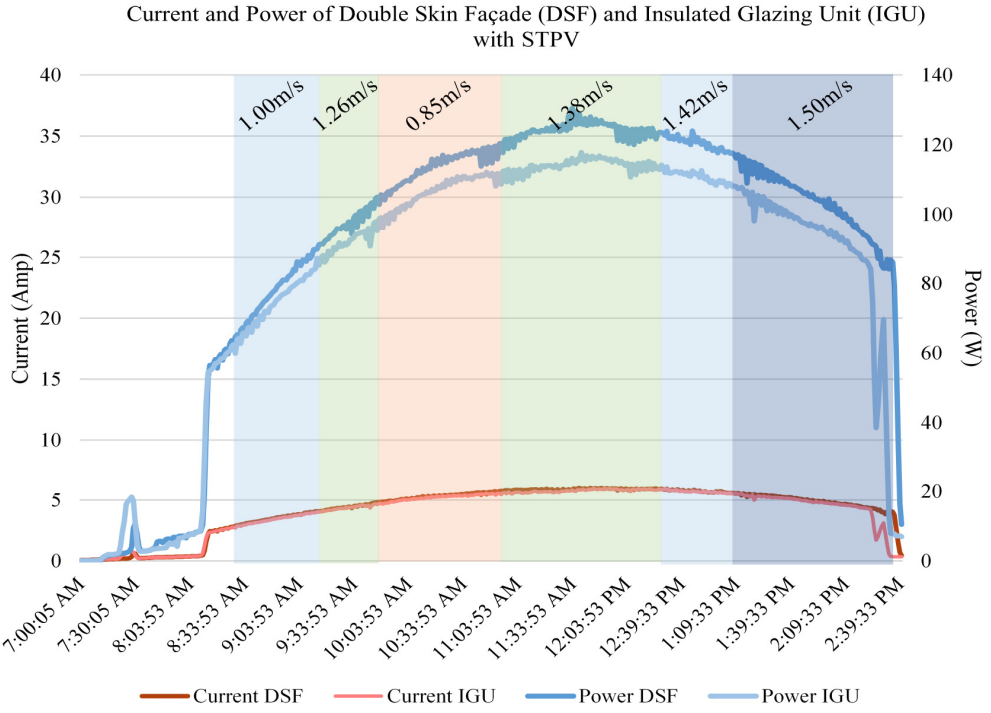

Figure 5 Power production and current of the STPV panels integrated on the DSF and the IGU on Day 1, with an average velocity within the cavity of approximately 1.25m/s.

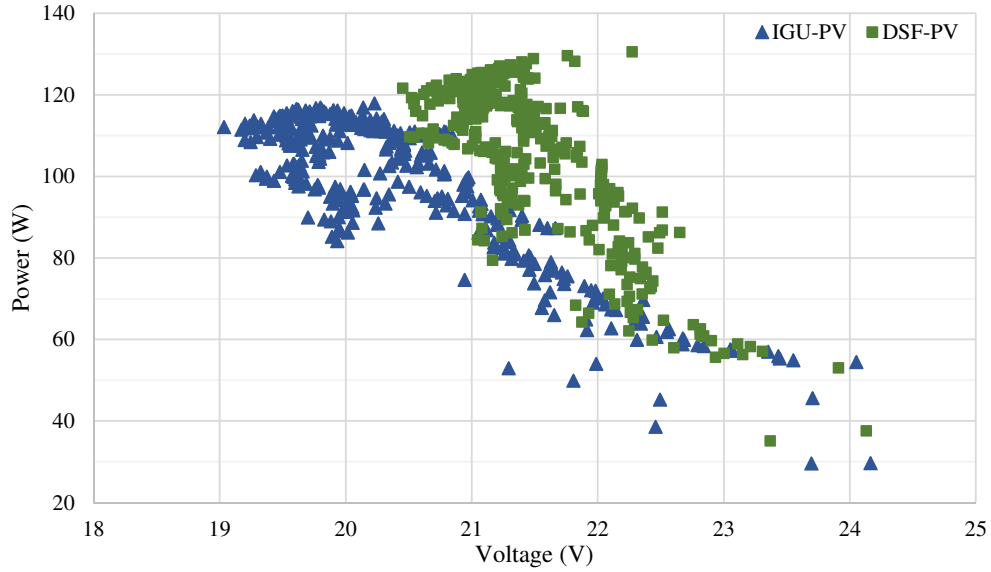

Figure 6 Power production of the STPV panels integrated on the DSF and the IGU in comparison to their voltage output on Day1, with an average velocity within the cavity of approximately 1.25m/s.

5. Conclusions

This study is focused on assessing the electrical performance of two similar STPV panels under the same exterior and interior conditions, integrated on different systems. An exterior experimental facility is set up to monitor the electrical performance of the STPV panel integrated on the exterior layer of a DSF and on an IGU, forming in this way a DSF-PV and an IGU-PV.

It should be noted, that the study presents some limitations. One of these is the short duration of the experiment. In the contrary, these days are around the September equinox and thus makes it easier for the results to be used for future studies and simulations. Also, the eight (8) monitored days that are presented in this manuscript are part of a longer experiment that is set-up to run for a whole year, in Montreal (Canada). Annual results can be later used, with more confidence to simulate IGU-PV and DSF-PV under different climatic conditions.

During the monitored days, the STPV integrated on the DSF out-performs the one integrated on the IGU. For all the eight (8) monitored days that the experiment lasted, the electrical performance of the DSF-PV presented increased values between 3% and 9% depending on the ventilation strategy of the cavity of the DSF-PV and the incident solar radiation. Even when the DSF-PV is not ventilated and acts as a buffer zone, the electrical performance of the STPV panels is 3% to 4.5% greater than this of the IGU-PV.

6. Acknowledgments

The authors would like to acknowledge the support of Unicel Architectural, Canadian Solar and the Hydro Quebec Industrial Chair.

7. References

Blue Sky Energy Inc. 2009. “SB3024i Datasheet.” Retrieved April 30, 2018 (http://www.blueskyenergyinc.com/uploads/pdf/SB3024(D)iL_Datasheet_(2017)_1.pdf).

Chen, Fangzhi, Stephen K. Wittkopf, Poh Khai Ng, and Hui Du. 2012. “Solar Heat Gain Coefficient Measurement

of Semi-Transparent Photovoltaic Modules with Indoor Calorimetric Hot Box and Solar Simulator." *Energy and Buildings* 53:74–84.

Chow, Tin Tai, Zhongzhu Qiu, and Chunying Li. 2009. "Potential Application Of 'see-Through' solar Cells in Ventilated Glazing in Hong Kong." *Solar Energy Materials and Solar Cells* 93:230–38.

TE Connectivity. 2005. "HSC100 METAL HOUSED POWER RESISTOR." Retrieved April 30, 2018 (http://www.te.com/commerce/DocumentDelivery/DDEController?Action=srchrtrv&DocNm=1625999&DocType=Customer+Drawing&DocLang=English).

Gaillard, Leon, Stéphanie Giroux-Julien, Christophe Ménézo, and Hervé Pabiou. 2014. "Experimental Evaluation of a Naturally Ventilated PV Double-Skin Building Envelope in Real Operating Conditions." *Solar Energy* 103:223–41.

Gaillard, Leon, Christophe Ménézo, Stéphanie Giroux, Hervé Pabiou, and Rémi Le-Berre. 2014. "Experimental Study of Thermal Response of PV Modules Integrated into Naturally-Ventilated Double Skin Facades." *Energy Procedia* 48:1254–61.

He, Wei et al. 2011. "Experimental and Numerical Investigation on the Performance of Amorphous Silicon Photovoltaics Window in East China." *Building and Environment* 46(2):363–69. Retrieved (http://dx.doi.org/10.1016/j.buildenv.2010.07.030).

Infield, David, Ursula Eicker, Volker Fux, Li Mei, and Jürgen Schumacher. 2006. "A Simplified Approach to Thermal Performance Calculation for Building Integrated Mechanically Ventilated PV Facades." *Building and Environment* 41(7):893–901.

Infield, David, Li Mei, and Ursula Eicker. 2004. "Thermal Performance Estimation for Ventilated PV Facades." *Solar Energy* 76(1–3):93–98.

James, P. A. B., M. F. Jentsch, and A. S. Bahaj. 2009. "Quantifying the Added Value of BiPV as a Shading Solution in Atria." *Solar Energy* 83(2):220–31.

Kapsis, Konstantinos and Andreas K. Athienitis. 2015. "A Study of the Potential Benefits of Semi-Transparent Photovoltaics in Commercial Buildings." *Solar Energy* 115:120–32. Retrieved (http://dx.doi.org/10.1016/j.solener.2015.02.016).

Liao, Wei and Shen Xu. 2015. "Energy Performance Comparison among See-through Amorphous- Silicon PV (Photovoltaic) Glazings and Traditional Glazings under Different Architectural Conditions in China." *Energy* 83:267–75. Retrieved (http://dx.doi.org/10.1016/j.energy.2015.02.023).

Mei, Li, David Infield, Ursula Eicker, and Volker Fux. 2003. "Thermal Modelling of a Building with an Integrated Ventilated PV Facade." *Energy and Buildings* 35(6):605–17.

Mei, Li, David Infield, Ursula Eicker, and Dennis Loveday. 2006. "Cooling Potential of Ventilated PV Facade and Solar Air Heaters Combined with a Desiccant Cooling Machine." 31:1265–78.

Miyazaki, T., a. Akisawa, and T. Kashiwagi. 2005. "Energy Savings of Office Buildings by the Use of Semi-Transparent Solar Cells for Windows." *Renewable Energy* 30:281–304.

MK Battery. 2015. "8A31DT AGM Battery." Retrieved April 30, 2018 (http://www.mkbattery.com/images/8A31DT.pdf).

National-Instruments. 2016. "NI 9213 Datasheet." Retrieved April 29, 2018 (http://www.ni.com/pdf/manuals/374916a_02.pdf).

National Instruments. 2016. "NI 9223 Datasheet." 1–12. Retrieved April 30, 2018 (http://www.ni.com/pdf/manuals/374223a_02.pdf).

Olivieri, L., E. Caamaño-Martin, F. Olivieri, and J. Neila. 2014. "Integral Energy Performance Characterization of Semi-Transparent Photovoltaic Elements for Building Integration under Real Operation Conditions." *Energy and Buildings* 68:280–91.

Park, K. E., G. H. Kang, H. I. Kim, G. J. Yu, and J. T. Kim. 2010. "Analysis of Thermal and Electrical Performance of Semi-Transparent Photovoltaic (PV) Module." *Energy* 35(6):2681–87.

Peng, Jinqing et al. 2016. “Numerical Investigation of the Energy Saving Potential of a Semi-Transparent Photovoltaic Double-Skin Facade in a Cool-Summer Mediterranean Climate.” *Applied Energy* 165:345–56.

Peng, Jinqing, Lin Lu, and Hongxing Yang. 2013. “An Experimental Study of the Thermal Performance of a Novel Photovoltaic Double-Skin Facade in Hong Kong.” *Solar Energy* 97:293–304.

Peng, Jinqing, Lin Lu, Hongxing Yang, and Tao Ma. 2015a. “Comparative Study of the Thermal and Power Performances of a Semi-Transparent Photovoltaic Façade under Different Ventilation Modes.” *Applied Energy* 138:572–83.

Peng, Jinqing, Lin Lu, Hongxing Yang, and Tao Ma. 2015b. “Validation of the Sandia Model with Indoor and Outdoor Measurements for Semi-Transparent Amorphous Silicon PV Modules.” *Renewable Energy* 80.

Qiu, Z. et al. 2009. “Performance Evaluation of the Photovoltaic Double Skin Facade.” *11th International IBPSA* 2251–57.

Riedon Inc. 2018. “Precision Current Resistor / DC Current Shunts.” Retrieved April 30, 2018 (https://riedon.com/media/pdf/RS.pdf).

Robinson, Leanne and Andreas Athienitis. 2009. “Design Methodology For Optimization Of Electricity Generation And Daylight Utilization For Façade With Semi-Transparent Photovoltaics.” *11th International IBPSA Conference, Building Simulation 2009* 811–18.

Tzempelikos, Athanassios and Andreas K. Athienitis. 2007. “The Impact of Shading Design and Control on Building Cooling and Lighting Demand.” *Solar Energy* 81(3):369–82.

Vartiainen, Eero. 2001. “Electricity Benefits of Daylighting and Photovoltaics for Various Solar Facade Layouts in Office Buildings.” *Energy and Buildings* 33:113–20.

Veitch, Jennifer A. and A. D. Galasiu. 2011. “The Physiological and Psychological Effects of Windows, Daylight and View at Home.” *National Research Council of Canada* 60.

Wang, Meng et al. 2017. “Comparison of Energy Performance between PV Double Skin Facades and PV Insulating Glass Units.” *Applied Energy* 194:148–60. Retrieved (http://dx.doi.org/10.1016/j.apenergy.2017.03.019).

Xu, Shen, Wei Liao, Jing Huang, and Jian Kang. 2014. “Optimal PV Cell Coverage Ratio for Semi-Transparent Photovoltaics on Office Building Façades in Central China.” *Energy and Buildings* 77:130–38.